PHYSICAL REVIEW E **68**, 031709 (2003)

Wetting properties of a hard-spherocylinder fluid on a substrate

D. de las Heras
Departamento de Física Teórica de la Materia Condensada, Universidad Autónoma de Madrid, E-28049 Madrid, Spain

L. Mederos
Instituto de Ciencia de Materiales, Consejo Superior de Investigaciones Científicas, E-28049 Cantoblanco, Madrid, Spain

E. Velasco
Departamento de Física Teórica de la Materia Condensada and Instituto de Ciencia de Materiales Nicolás Cabrera,
Universidad Autónoma de Madrid, E-28049 Madrid, Spain

(Received 17 June 2003; published 26 September 2003)

A density-functional theory is used to analyze the wetting properties of a fluid made up of hard spherocylinders of a length-to-breadth ratio $L/D=5$ on a model substrate. The substrate imposes an exclusion boundary condition over the molecular centres of mass, while at the same time favoring a definite molecular orientation, either parallel or perpendicular to the substrate, in a region next to the substrate. The wetting properties of this system are seen to depend on the strength with which the substrate orients the molecules: as the latter is increased, wetting by nematic phase is followed by a region of partial wetting which then leads to reentrant wetting by nematic. The two wetting transitions correspond to wetting films with nematic director perpendicular and parallel to the substrate, respectively. Also, in the region of partial wetting, an anchoring transition occurs in the substrate-nematic interface between two different director configurations (parallel and perpendicular to the substrate). Finally, a metastable wetting transition by isotropic is also obtained. This model considerably enriches the wetting phenomenology of the hard-spherocylinder fluid on substrates, of which only the pure hard wall, with no surface control parameter available, has been considered so far.

DOI: 10.1103/PhysRevE.68.031709 PACS number(s): 64.70.Md, 61.30.Cz, 61.30.Hn

I. INTRODUCTION

The microscopic understanding of the surface properties of liquid crystals are crucial in the design of liquid-crystal based devices and the optimization of their response. These properties depend very sensitively on a number of effects occurring at the interface, which are ultimately linked to the molecular interactions and the interactions with the surface. A number of analyses have been published in the past few years which are based on phenomenological Landau–de Gennes–type theories [1–4]. These studies have been of enormous interest since they have shown the basic surface phenomenology that can be expected and how different phenomena such as wetting and anchoring are linked.

Some effort has also been expended in constructing simple molecular models that not only contain the molecular interactions explicitly, but also incorporate the coupling between the density and the orientational order parameter. These models have been shown to contain the basic phenomenology. Most of these models rely on explicit soft anisotropic interactions treated in mean field while hard-core repulsive interactions are grossly approximated by hard spheres. More realistic models, e.g., the Gay-Berne model, have begun to be studied by simulation [5].

Also, the surface properties of purely repulsive models such as hard ellipsoids or hard spherocylinders (HSPCs) have been studied by simulation [6,7] and by Onsager theory [6–9]. These models are very interesting since hard-core interactions are believed to be very important in establishing bulk liquid-crystalline order, and it is natural to ascertain to what extent these models are also sensible to study interfacial properties. In this respect, the standard model is the HSPC fluid against a purely hard wall. Early studies by Poniewierski and Holyst [8], based on an extension of Onsager theory to inhomogeneous distributions, gave some evidence for complete wetting by nematic phase of the wall-isotropic interface. This evidence has been increased by more recent work using a Zwanzig approximation [10] of the extended Onsager theory [11] and by a computer simulation study [12]. However, the HSPC fluid against a hard-wall model does not have the flexibility to show other possible surface behaviors of the HSPC fluid. Thus, none of the above studies have focused on the specific wetting properties that might be obtained if one considers not a simple hard wall but different types of substrates with specific interactions, favoring one of the phases that coexist in bulk, either isotropic or nematic, or showing a preferred orientation of the molecules at the substrate.

In this paper we have used a standard Onsager-type density-functional theory, extended to include general spatially inhomogeneous phases, to examine the wetting properties of a HSPC fluid against a model surface. The model surface is flexible enough so that one can modify its affinity toward different types of fluids. The amount of surface nematic order can change as the result of variations in the surface strength parameter contained in the model surface potential, and this can modify the wetting or nonwetting properties of the fluid. In fact we have found an extremely rich phenomenology, with wetting behaviors of a different nature coexisting with an anchoring transition whereby the nematic director undergoes a phase transition between parallel and homeotropic alignment. In this way we have demonstrated,

1063-651X/2003/68(3)/031709(10)/$20.00

in particular, the interplay between wetting and anchoring properties in a well-defined molecular model.

The remainder of this paper is organized as follows. In the following section we give a short account of the theoretical scheme. In Sec. III we present some details of the numerical calculations together with the results, followed in Sec. IV by some conclusions and some directions for future work.

II. THEORY

A detailed account of the theory has been presented elsewhere [13–15]. Here we only sketch briefly the main ingredients and the numerical approach. The relevant free energy for our adsorption problem is the surface tension or surface free energy γ which, in the grand canonical ensemble, can be expressed as the excess (over bulk) grand potential Ω per unit transverse area A:

$$\gamma=\frac{\Omega-\Omega_b}{A}=\frac{\Omega+PV}{A}, \quad \Omega=F-\mu N, \tag{1}$$

where F is the Helmholtz free energy, P the pressure, V the volume, μ the imposed chemical potential, Ω_b the grand potential of the bulk phase, and N the number of molecules. In the present work we use an extension of Onsager theory to obtain the Helmholtz free energy, which is the central quantity to approximate. Onsager theory [16], which is a second-virial approximation, was proposed to investigate the bulk isotropic-nematic phase transition in a system of long hard rods. It was later extended [17,18] to incorporate some effects of spatial correlations, which improves the coexistence densities of the bulk isotropic-nematic transition.

Here we further extend the theory to allow for slowly varying molecular distributions of the type that are expected in a liquid-crystal-forming material near the isotropic-nematic transition and close to a substrate. If $\rho(z,\hat{\mathbf{\Omega}})$ is the one-molecule distribution function of the fluid [with $\rho(z,\hat{\mathbf{\Omega}})d^3rd\hat{\mathbf{\Omega}}$ giving the average number of molecules in a volume element d^3r at a distance z from the substrate and with orientation $\hat{\mathbf{\Omega}}$ within the solid angle $d\hat{\mathbf{\Omega}}$], the Helmholtz free-energy density functional is approximated by

$$\begin{aligned}F[\rho]=F_{\rm id}[\rho]+kT\int\int d\mathbf{r}d\hat{\mathbf{\Omega}}\rho(z,\hat{\mathbf{\Omega}})\\ \times\left[\frac{\Delta\Psi(\rho(z))}{\frac{4\pi}{3}\rho(z)\sigma_{\rm eq}^3}\right]\int\int d\mathbf{r}'d\hat{\mathbf{\Omega}}'v_{\rm exc}(\mathbf{r}-\mathbf{r}',\hat{\mathbf{\Omega}},\hat{\mathbf{\Omega}}')\\ \times\rho(z',\hat{\mathbf{\Omega}}')+\int d\mathbf{r}d\hat{\mathbf{\Omega}}\rho(z,\hat{\mathbf{\Omega}})v_{\rm ext}(z,\hat{\mathbf{\Omega}}),\end{aligned} \tag{2}$$

where $v_{\rm exc}$ is the overlap function for two HSPCs (unity if they overlap and zero otherwise), $\Delta\Psi(\rho(z))$ is a prefactor (see later) that depends on the angular-averaged density distribution $\rho(z)$,

$$\rho(z)\equiv\int d\hat{\mathbf{\Omega}}\rho(z,\hat{\mathbf{\Omega}}), \tag{3}$$

$v_{\rm ext}$ is the external potential representing the effect of the substrate on a single molecule, and $\sigma_{\rm eq}$ is an effective molecular diameter that will be discussed at the end of this section (see also Refs. [13–15]). We choose the z axis to be normal to the substrate. Then our density distributions $\rho(z,\hat{\mathbf{\Omega}})$ only depend on that coordinate since the substrate is chosen not to possess any transverse structure. This form for the intrinsic free energy is a simplification of the Somoza-Tarazona density functional [13], which was proposed to deal with highly structured density distributions and contains an averaged density distribution over molecular interactions; here, for the sake of simplicity, this averaged density distribution is taken to be simply the local density distribution since we do not expect highly inhomogeneous density profiles. Thus, the theory is not exactly the simple extension of the Onsager theory (which amounts to approximating the density factor between squared brackets by a constant factor 1/2), first used by Holyst and Poniewierski [19]. Alternatively it can be viewed as a generalization of the extended Onsager theory due to Parsons [17] and Lee [18] to inhomogeneous systems. In any case, because of the relatively smooth density distributions, we expect to obtain similar results by use of any of the versions of density-functional theory. In this connection, it is to be noted that the simple Onsager density-functional form, as proposed by Holyst and Poniewierski [19], has been compared to simulation [6] for the case of hard ellipsoids of revolution against a model hard wall, and shown to reproduce the simulation results quite reasonably.

$F_{\rm id}[\rho]$ is the ideal-gas free-energy density functional which is exactly given by

$$F_{\rm id}[\rho]=kT\int d\mathbf{r}d\hat{\mathbf{\Omega}}\rho(z,\hat{\mathbf{\Omega}})[\ln\rho(z,\hat{\mathbf{\Omega}})-1], \tag{4}$$

with T as the temperature and k Boltzmann's constant. As usual we introduce an angular distribution function $f(z,\hat{\mathbf{\Omega}})$ BY $\rho(z,\hat{\mathbf{\Omega}})=\rho(z)f(z,\hat{\mathbf{\Omega}})$ and work not with the function itself but with the first moments relevant for axisymmetric molecules:

$$\eta_m(z)=\int d\hat{\mathbf{\Omega}}f(z,\hat{\mathbf{\Omega}})Y_{2m}(\hat{\mathbf{\Omega}}), \quad m=0,\pm 1,\pm 2, \tag{5}$$

with Y_{lm} as a spherical harmonic. Assuming mirror symmetry with respect to the xz plane, the only significant moments are three: transforming to a reference frame where the new z axis lies along the local director the three relevant moments are $\psi(z)$, the angle between the director $\hat{\mathbf{n}}$ and the unit vector normal to the substrate $\hat{\mathbf{z}}$, and two distributions that represent the ordering around the local director: $\eta(z)$ (uniaxial order parameter) and $\sigma(z)$ (biaxial order parameter). These order-parameter functions, together with the local density $\rho(z)$, define the configurational state of our adsorption system. Details on how the free energy is calculated in terms of these order parameters can be obtained from Refs. [13–15]. Here we only note that, once the external potential representing the effect of the substrate is specified, the resulting surface-tension functional $\gamma([\rho];\mu)$ can be minimized numerically with respect to the four order-parameter distributions, for fixed bulk conditions, i.e., for fixed chemical potential μ (T is not a relevant thermodynamic variable since our molecular model is hard).

The external potential has been modeled according to the expression

$$v_{\text{ext}}(z,\hat{\mathbf{\Omega}})=\begin{cases}\infty, & z<0\\ V_0 e^{-\alpha z}P_2(\hat{\mathbf{\Omega}}\cdot\hat{\mathbf{z}}), & z\geqslant 0,\end{cases} \tag{6}$$

where P_2 is a second-order Legendre polynomial. This choice for external potential has interesting implications for the director configuration that the nematic fluid is going to prefer. First, note that the spatial part of the external potential affects only the centers of mass of the spherocylinders and that, accordingly, the external potential (6) is not a purely hard wall. As far as the orientation of the molecules is concerned, the presence of the Legendre polynomial favors parallel alignment, i.e., tilt angle $\psi=90°$ at the substrate, when V_0 is positive, and homeotropic alignment, $\psi=0°$, when the parameter V_0 is negative.

A similar external potential was used by Allen [6,7] in his work on nematic films of hard ellipsoids, the only difference being that the spatial extent of the potential from the susbtrate was controlled by a step function up to a distance of half the length of an ellipsoid. Since our external potential contains a free parameter, the strength parameter V_0 modeling the orienting properties of the substrate, a range of different phenomena can be covered by changing the value of the strength parameter. In addition, it has some other advantages over a purely hard wall from a computational point of view; in particular, spatial and orientational coordinates are decoupled, and the contribution to the free energy from the external potential can be greatly simplified. By contrast, in a purely hard-wall potential spatial and orientational coordinates are fully coupled and this complicates significantly the free-energy expression, in particular, the intrinsic contribution, where different overlap regions have to be identified, and also the entropic contribution.

Since the interaction model does not possess an intrinsic energy scale, energy units are chosen as kT. The length unit is taken to be σ_{eq}, the equivalent hard-sphere diameter. An equivalent hard-sphere system arises in the model through the expression for the function $\Delta\Psi$, which is the Carnahan-Starling expression for the free-energy per particle and unit thermal energy of a fluid of hard spheres. This function depends on the packing fraction of an equivalent system of hard spheres, which is chosen to be equal to the packing fraction of the actual system of HSPC [13–15]. For the molecules chosen in this study, with $L/D=5$, the value of the equivalent hard-sphere diameter is $\sigma_{\text{eq}}=2.04D=0.41L$.

Before showing the results it is worth pointing out an issue concerning the violation of an exact sum rule by the density functional. Since our external potential represents a hard-wall boundary for the molecular centers of mass there exists a simple sum rule [20], $P/kT=\rho(0)$, which relates the pressure P to the value of the local number density right at the susbtrate, $\rho(0)$. Density-functional approximations that do not incorporate an averaged density cannot satisfy this sum rule [21], and for this reason the Onsager model and the version used in this work fail to satisfy the rule. We believe this is not a serious shortcoming of the model, since in the present context we are interested in orientation properties and orientational wetting phenomena, and the use of a more sophisticated density functional, like the one proposed by Somoza and Tarazona [13], would not change qualitatively the conclusions of the present work.

III. RESULTS

In the following we restrict ourselves to considering hard spherocylinders with a length-to-breadth ratio $L/D=5$. Let us first discuss the effect of the external potential (6) on the positional and orientational order of an adsorbed nematic film, since the understanding of the behavior of the nematic film for a particular value of the surface potential strength will be crucial to analyze the results obtained when probing the surface behavior of the system close or at the bulk isotropic-nematic phase transition, i.e., the wetting behavior of the system.

The potential can be regarded to have two components: one affects the molecular centers of mass by forbidding configurations where the centers of mass are at $z\leqslant 0$. The other affects the orientations of the molecules and is governed by the strength parameter V_0. Note that $V_0=0$ does not correspond to a hard wall, since our wall is hard *only* as far as the centers of mass are concerned. This difference crucially affects any comparison with the computer simulation results of Dijkstra *et al.* [12] who used a purely hard wall.

The parameter V_0 can be positive or negative. If positive, the favored molecular orientation is parallel to the wall whereas, if negative, molecules tend to orient perpendicular to the wall. However, the component affecting the centers of mass always favors perpendicular alignment, since in this way molecules can pack more densely right at the substrate. This is in sharp contrast with the molecular configuration adopted by HSPC against a *hard* wall, which is parallel to the substrate [9,12,22–24] (the same packing effect, favoring homeotropic alignment, has been observed by Allen [6,7] in his study of hard ellipsoids against model walls using a similar external potential). Then, for $V_0<0$, the external potential favors homeotropic alignment. When $V_0>0$, but not very high, both effects compete but packing imposes its preferred orientation, the favored alignment being still homeotropic. Finally, if V_0 is positive and large (larger than a value of order kT), alignment changes to parallel since the orienting surface term can impose its preferred orientation. The value of V_0 where the favored alignment changes depends weakly on the range parameter α.

To illustrate these different scenarios we have plotted in Fig. 1 a number of profiles for nematic and isotropic phases in contact with the substrate. We show the density, director configuration, and order around the local director for the corresponding interface. We emphasize that the order parameters are referred to a reference frame tied to the local director, the *proper* frame, not to the *lab* frame associated with the (fixed) substrate which is sometimes used. Unless otherwise

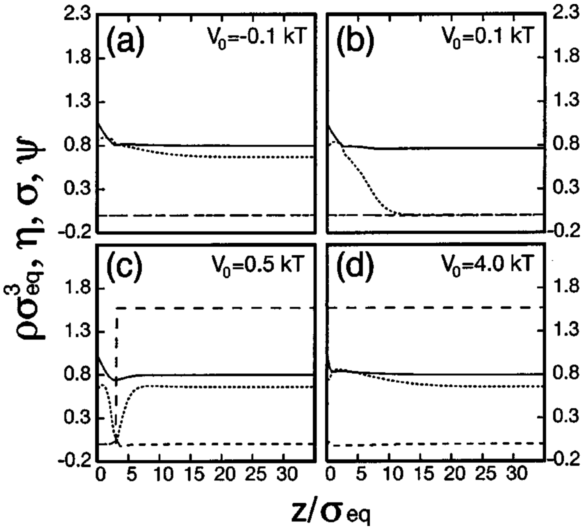

FIG. 1. Order-parameter profiles for a system of hard spherocylinders at isotropic-nematic coexistence ($\mu=\mu_{\rm coex}$) and for different values of the surface strength parameter V_0. The surface potential decay inverse length is taken to be $\alpha=0.3\sigma_{\rm eq}^{-1}$. ρ is the number density (continuous lines) in units of $\sigma_{\rm eq}$, η the uniaxial nematic order parameter (dotted lines), σ the biaxial nematic order parameter (short dashed lines), and ψ the tilt angle of the director (long dashed lines), expressed in radians. All profiles refer to the same vertical scale. In parts (a) and (b) the biaxial order parameter and the tilt-angle profiles are zero so that they appear as a single horizontal line.

noted, all profiles and results pertaining to the present work correspond to a value $\alpha=0.3\sigma_{\rm eq}^{-1}$. The system is prepared in each case by placing the director either parallel or perpendicular to the substrate and with a corresponding boundary condition far from the substrate (the distance between this boundary and the substrate was taken typically to be $30\sigma_{\rm eq}$ but, when studying wetting phenomena, much larger distances were sometimes necessary). The density and uniaxial order-parameter profiles were initialized to constant bulk values (consistent with the chemical potential) whereas the biaxial order parameter profile was taken to be zero. The density functional was then minimized using a conjugate-gradient technique and the minimum surface free-energy configuration was chosen as the equilibrium configuration, which in each case corresponds to the profiles plotted in the figure. The equilibrium structure is reached typically in 50 iterations using the convergence criterion such that the norm of the gradient be less than 10^{-3}. Figure 1 includes four cases corresponding to four different values of V_0. In all cases the density profiles are very smooth, but close to the substrate the density rises quite significantly to a value higher than the bulk value. The extent of the resulting adsorbed film is typically equal to half a molecular length (see later). Before discussing the behavior of the order-parameter profiles, we note that since they are referred to the proper reference frame, there exists a trivial degeneracy implying that a given orientational state can be specified by two equivalent sets of order parameters (η,σ) and (η',σ') related by

$$\eta=-\tfrac{1}{2}\eta'+\tfrac{3}{4}\sigma', \quad \sigma=\eta'+\tfrac{1}{2}\sigma'. \tag{7}$$

We have always applied the transformation is such a way as to have positive values of the uniaxial order parameter η.

In Fig. 1(a) V_0 is negative, and the director exhibits homeotropic alignment; a small order parameter adsorption can be seen near the substrate, and the biaxial order parameter is zero as it corresponds to a uniaxial phase. In Fig. 1(b), where bulk conditions were chosen to correspond to an isotropic phase, V_0 is positive, but not so strong as to orient the director parallel to the substrate. Again, the system has uniaxial symmetry. As V_0 is increased, Fig. 1(c), there appears a region where the uniaxial order parameter becomes depleted, going to (almost) zero. On going across this region the director orientation changes rapidly from perpendicular to parallel. The thickness of the first layer, where molecules lie perpendicular to the substrate, as obtained by the width of the uniaxial order-parameter profile at half height, is $\delta=2.1\sigma_{\rm eq}=0.86L$, i.e., it corresponds approximately to a one-molecule-thick layer. This width coincides with the extent of the adsorption layer as obtained from the density profile. As far as orientational properties are concerned, the layer is largely decoupled from the rest of the film. Its existence is the result of the dispersion, orientational-dependent part of the potential having a slightly larger range ($\alpha^{-1}\sim 3\sigma_{\rm eq}$) than packing effects caused by the hard component of the susbtrate interaction, which are located right at the substrate.

Finally, when V_0 is sufficiently high such that the angular part of the surface potential is successful in orienting all the molecules parallel to the substrate, including the first layer, the orientation of the film becomes uniformly parallel, as shown in Fig. 1(d), and the first layer disappears altogether. It is interesting to compare these profiles with those obtained by Allen [6,7], who does not report the type of profiles shown in Fig. 1(c)—including a defect in the form of a sharp discontinuity in the director orientation. One of the possible reasons is the use by Allen of a strictly step function, with a width equal to half the molecular length of an ellipsoid; another reason could be the strong anchoring conditions used by Allen ($V_0/kT=3.3$ in our language). In any case, we also find smooth profiles, together with a small adsorption right at the substrate.

An interesting question concerns the appearance of biaxiality in the order-parameter distributions. Recently, Poniewierski has shown [9] that the parallel-aligned HSPC fluid against a purely hard wall is biaxial even for bulk conditions well inside the isotropic density stability range. It is natural to expect that this result can apply as well in our system, where coexistence conditions prevail. Indeed, the very fact that a tilt angle can be calculated at all for the conditions shown in Figs. 1(c),(d) demonstrates that the corresponding profiles are biaxial. Since we have adopted a reference frame associated with the local director, the small value of the biaxial order-parameter profiles in Figs. 1(c),(d) only indicates a weak departure of the orientational distribution from complete azimuthal symmetry around the local, parallel-aligned director.

A. Wetting transitions

We now discuss the occurrence of wetting transitions. Since we are considering isotropic-nematic coexistence (we have left aside altogether the possibility of smectic formation in our system), wetting may be of two types: either a macroscopically thick nematic film intrudes between the substrate and a bulk isotropic phase (wetting by nematic) or a macroscopically thick isotropic film interposes between the substrate and a bulk nematic phase (wetting by isotropic). Situations where films are of finite (microscopic) width will be termed nonwetting or partial wetting. As explained later in this section, we have found two wetting transitions associated to the value of the surface strength parameter V_0: as this parameter is increased, the system goes from a situation of complete wetting by a nematic phase with the director perpendicular to the substrate, to a situation of partial wetting, and finally a *reentrant wetting* where the nematic director lies parallel to the susbtrate. Also, in the parameter region where partial wetting obtains, an anchoring transition between states with different director orientations is found, together with a metastable wetting transition by the isotropic phase. Before discussing this phenomenology we briefly mention how the different transitions were located.

In order to locate wetting transitions we have conducted a series of numerical minimizations using different boundary conditions in bulk. The bulk chemical potential is set to the coexistence value $\mu=\mu_{\mathrm{coex}}$, a boundary condition at bulk is chosen (either isotropic or nematic), and the strength substrate parameter V_0 is varied. Surface free energies $\gamma_{SN}(V_0)$ and $\gamma_{SI}(V_0)$ for the substrate-nematic (SN) and the substrate-isotropic (SI) interfaces are then calculated by numerically minimizing the surface free energy using nematic and isotropic boundary conditions in bulk, respectively [25]. Since we are considering the possibility that the director configuration may adapt itself to the boundary and thermodynamic conditions imposed by choosing the minimum surface free-energy configuration, we have to anticipate the occurrence of nematic films with different director configurations in bulk, either parallel ($\gamma_{SN}^{\parallel}$) or perpendicular ($\gamma_{SN}^{\perp}$) to the substrate. The surface free energy for the isotropic-nematic interface, γ_{IN}, is calculated beforehand and only once, since it is a free interface and consequently its surface tension does not depend on V_0. As is well known, the equilibrium director configuration of the free-nematic-isotropic interface of a HSPC fluid corresponds to a director parallel to the interface [9,15,22–24]. However, as discussed below, we will have to use two values for γ_{IN}: one for the equilibrium free interface, called $\gamma_{IN}^{\parallel}$, and another for a *nonequilibrium* free interface where the director lies perpendicular to the interface, called $\gamma_{IN}^{\perp}$; the latter quantity will be necessary when the nematic-isotropic interface be sufficiently close to a substrate-nematic interface favoring strong homeotropic anchoring conditions, which will then propagate to the nematic-isotropic (NI) interface. The values obtained for these two quantities are [15] $\gamma_{IN}^{\parallel}=0.0433\sigma_{\mathrm{eq}}^{-2}kT$ and $\gamma_{NI}^{\perp}=0.0533\sigma_{\mathrm{eq}}^{-2}kT$. Antonow's rule then gives the contact angle θ of the isotropic-nematic (IN) interface with respect to the substrate when there is an isotropic phase in bulk as

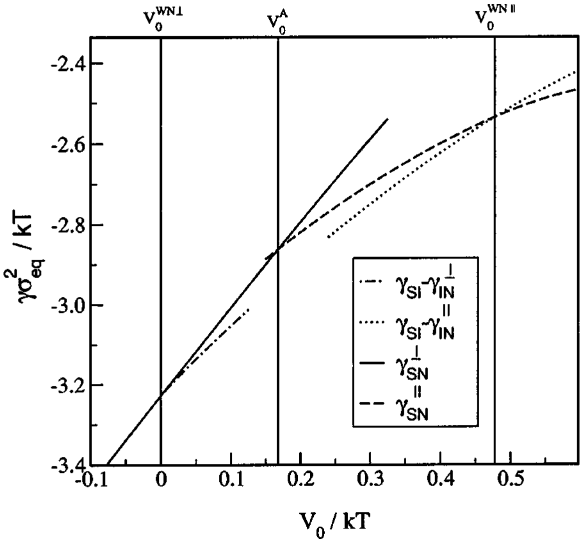

FIG. 2. Surface tensions γ of the different interfaces as a function of surface strength parameter V_0. The surface potential decay inverse length is taken to be $\alpha=0.3\sigma_{\mathrm{eq}}^{-1}$. The surface tensions for the different interfaces ($\gamma_{SN}^{\parallel}$ for the substrate-nematic interface with the director oriented parallel to the substrate, $\gamma_{SN}^{\perp}$ for the substrate-nematic interface with the director oriented perpendicular to the substrate, γ_{SI} for the substrate-isotropic interface, and $\gamma_{IN}^{\parallel}$, $\gamma_{NI}^{\perp}$ for the nematic-isotropic interface with the director parallel and perpendicular to the interface, respectively) are represented by lines, as indicated in the key box. The appropriate nematic-isotropic surface tension is subtracted from γ_{SI} to permit easier visualization of the wetting transitions, indicated in the upper part of the panel by $V_0^{WN\parallel}$ and $V_0^{WN\perp}$. The anchoring transition is indicated by V_0^{A}.

$$\gamma_{SI}=\gamma_{SN}+\gamma_{IN}\cos\theta \quad \text{(partial wetting by nematic).}$$

When $\theta=0$ then wetting by the nematic phase occurs since it is more favorable for the system to interpose a nematic film of macroscopic thickness between the substrate and the bulk isotropic phase:

$$\gamma_{SI}=\gamma_{SN}+\gamma_{IN} \quad \text{(wetting by nematic).}$$

In contrast, when nematic conditions prevail in bulk the contact angle θ' of the IN interface with respect to the substrate is given by

$$\gamma_{SN}=\gamma_{SI}+\gamma_{IN}\cos\theta' \quad \text{(partial wetting by isotropic),}$$

and the condition $\theta'=0$ indicates a transition to wetting by the isotropic phase where an isotropic film of macroscopic thickness intrudes between the substrate and the bulk nematic phase:

$$\gamma_{SN}=\gamma_{SI}+\gamma_{IN} \quad \text{(wetting by isotropic).}$$

To illustrate how the wetting transitions are located using the above wetting conditions we present in Fig. 2 the surface tensions of the SI and SN interfaces as a function of V_0; we have added (subtracted) to the latter (former) the

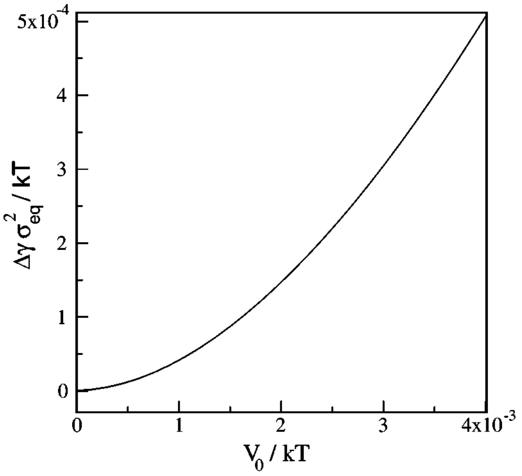

FIG. 3. Difference in surface tensions $\Delta\gamma=\gamma_{SN}^{\perp}+\gamma_{IN}^{\perp}-\gamma_{SI}$ against value of surface strength parameter V_0 in the region of partial wetting by nematic but close to the wetting transition. The curve is a fit of density-functional data to a quadratic polynomial. The surface potential decay inverse length is taken to be $\alpha=0.3\sigma_{\rm eq}^{-1}$.

V_0-independent value of $\gamma_{IN}^{\parallel}$ or $\gamma_{NI}^{\perp}$ in order to visualize more easily how the crossing of the different free energies takes place.

1. Wetting by a nematic phase with director perpendicular to the substrate

The condition $\gamma_{SI}=\gamma_{SN}^{\perp}+\gamma_{IN}^{\perp}$ (corresponding to a uniform, perpendicular tilt director configuration) is met at $V_0=V_0^{WN\perp}\equiv 0$ (see Fig. 2), signaling the occurrence of wetting by a nematic film with a director aligned perpendicular to the substrate (tilt angle $\psi=0°$). The two members of the above equality become equal at the transition, but they appear to do so tangentially which indicates that the transition is presumably of second order or maybe weakly of first order. Further evidence is obtained by the impossibility to generate metastable states, i.e., nematic films of finite width for $V_0<V_0^{WN\perp}$. In order to investigate this question in more detail we have computed surface free energies for values $V_0>V_0^{WN\perp}$ but close to the wetting transition, and checked that $\Delta\gamma\equiv\gamma_{SN}^{\perp}+\gamma_{IN}^{\perp}-\gamma_{SI}\sim(V_0-V_0^{WN\perp})^2$, with no linear dependence (Fig. 3). Therefore, within the accuracy of our calculations, we may say that this wetting transition is probably of second order.

This conclusion is supported by a parallel analysis based on partial minimizations of the functional. The idea consists of performing constrained minimization where the width of the nematic layer, L (a slow variable of the problem), is not allowed to change, while the remaining variables are relaxed. Here we assume a uniform value of the tilt angle across the wetting layer, an assumption that, for very thick wetting nematic layers, i.e., very close to the wetting transition, will necessary fail (see discussion later on). In no case does the resulting constrained surface free-energy difference $\Delta\gamma(L)\equiv\gamma_{SI}^{*}(L)-\gamma_{SN}^{\perp}-\gamma_{NI}^{\perp}$ [$\gamma_{SI}^{*}(L)$ being the surface free energy for the constrained SI interface] show any barrier separating a layer with finite width from a wetting layer of infinite width, which would be a signal of a first-order phase transition.

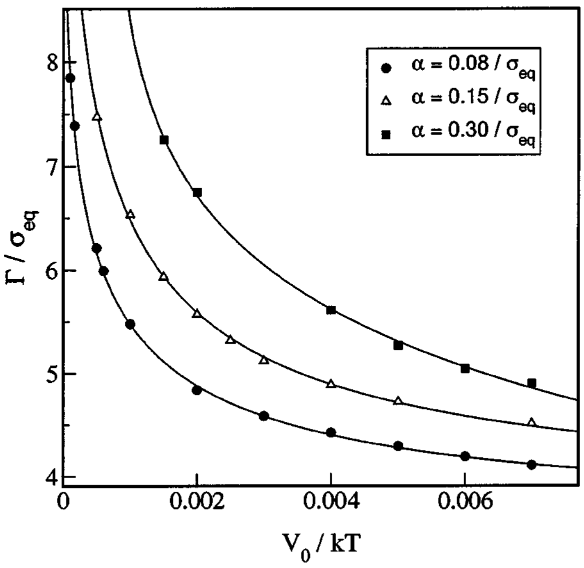

FIG. 4. Nematic adsorption Γ vs surface strength parameter V_0 for various values of the surface inverse decay length α. The data are associated to the wetting transition at $V_0^{WN\perp}$ of a nematic with the director aligned perpendicular to the substrate. Symbols are calculations with the density functional. Continuous lines are fits to the form $\Gamma=a+b\ln(V_0/kT-c)$.

A useful quantity to characterize nematic adsorption is the integrated uniaxial orientational order-parameter profile

$$\Gamma=\int_0^{\infty}dz\,\eta(z), \tag{8}$$

which gives an indication of how thick the nematic layer is. The nematic-adsorption parameter obviously depends on the chemical potential μ and the surface strength parameter V_0. The behavior of Γ at $\mu=\mu_{\rm coex}^{-}$ (i.e., with isotropic conditions at bulk) as the wetting transition is approached from above, $V_0\to(V_0^{WN\perp})^{+}$, can be used to ascertain the nature of the wetting transition: at a first-order transition Γ would jump from a finite to an infinite value, whereas if the transition is continuous the nematic adsorption would increase in a continuous fashion and ultimately diverge at the transition. Computing Γ requires obtaining *truly* equilibrium distribution profiles. Since Γ is directly related to L, the thickness of the nematic layer, it is a slow variable. In order to calculate Γ for a fixed value of V_0 we have followed the technique mentioned in the preceding paragraph, searching for an approximate value of L by first doing short minimization runs and then refining this initial guess by full minimizations. The nematic-adsorption parameter, plotted in Fig. 4, always shows a continuous growth as the wetting transition is approached. The parameter has been plotted for different values of α, the range parameter of the surface potential, covering ranges between $3.3\sigma_{\rm eq}$ and $12.5\sigma_{\rm eq}$. This again confirms the continuous nature of the wetting transition (we cannot rule out, however, the possibility that for other values of α or

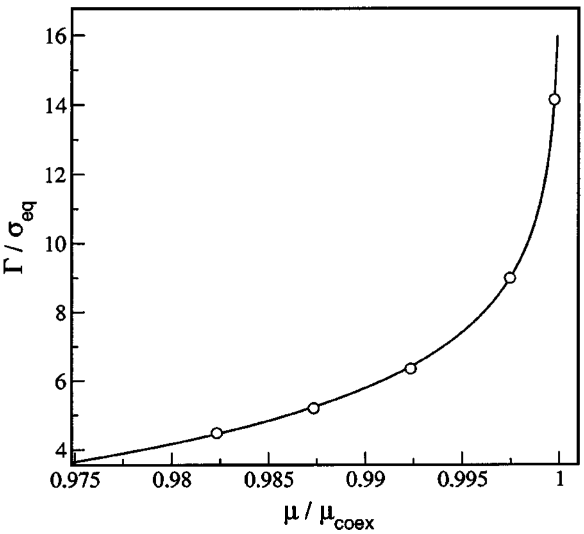

FIG. 5. Nematic-adsorption Γ vs chemical potential μ relative to the coexistence value μ_{coex} for a substrate strength parameter $V_0 = -0.1kT$ and a surface potential decay inverse length $\alpha = 0.3\sigma_{\text{eq}}^{-1}$ to the substrate. The data are associated to the wetting transition at $V_0^{WN\perp}$ of a nematic with the director aligned perpendicular to the substrate. Symbols are calculations with the density functional. Continuous lines are fits to the form $\Gamma = a + b\ \ln(\mu/\mu_{\text{coex}} - c)$.

functionally longer-ranged surface potentials the transition may change its order). Corresponding to short-range intermolecular interactions, the nematic-adsorption parameter shows logarithmic growth as the wetting transition is approached at coexistence. This is supported by fits to the form $\Gamma = a + b\ \ln(x-c)$, with $x = V_0/kT$; a, b, and c are fitting parameters that depend on the value of α. The values of a vary between $-0.5\sigma_{\text{eq}}$ and $-1.0\sigma_{\text{eq}}$, whereas b is around $-0.9\sigma_{\text{eq}}$. The parameter c is always nearly zero (10^{-5}–10^{-4}).

In Fig. 5 the nematic-adsorption parameter is plotted for a fixed value of the strength parameter $V_0 = -0.1kT < V_0^{WN\perp}$, and increasing chemical potential $\mu \rightarrow \mu_{\text{coex}}^{-}$. The divergence of Γ supports the complete wetting scenario. Again, the data clearly show a logarithmic-type divergence of the adsorption. The fitting form is $\Gamma = a + b\ \ln[(c-x)/x]$, with $x = \mu/\mu_{\text{coex}}$, and we obtain $a = -5.00\sigma_{\text{eq}}$, $b = 2.34\sigma_{\text{eq}}$, and $c = 1.00$. Given the elusive character of the prewetting transition, the absence of a discontinuity in Γ, which would signal the existence of a prewetting transition, does not rule out first-order wetting but simply supports evidence for the continuous character of this wetting transition collected by other means.

The location of the wetting transition, i.e., the value of V_0 at which the nematic phase ceases to wet the substrate, $V_0^{WN\perp}$, is in general very small but depends weakly on the value of the range parameter α. Provided the transition is of second order, a simple model based on the Fowler approximation predicts a value $V_0^{WN\perp} = 0$ for $\alpha < 0.63\sigma_{\text{eq}}^{-1}$ and $V_0^{WN\perp} > 0$ for $\alpha > 0.63\sigma_{\text{eq}}^{-1}$. Exact minimizations of the functional are not accurate enough to precisely locate the wetting transition, but our approximate analysis gives results in agreement with the Fowler approximation.

The nematic fluid forming the wetting layer is subject to two different boundary conditions: at the substrate the favored configuration corresponds to the molecules arranged perpendicular to the substrate (since $V_0 \sim 0$ this is due to packing effects), whereas a free-isotropic-nematic interface favors parallel alignment of the director. Clearly, the only manner in which these two conditions can be met is when the director rotates uniformly across the wetting layer, which implies an elastic energy. This situation has been studied previously by Sullivan and Lipowsky [26] and by Sluckin and Poniewierski [27], using an effective interfacial approach, and by Braun *et al.* [28] in the context of a Landau–de Gennes free-energy functional. For an emergent, thick wetting nematic layer, a distorted-tilt director configuration satisfying both boundary conditions but incurring an elastic energy should indeed occur, and this would modify the location of the wetting transition and bring about a crossover to a different growth law for the layer thickness as coexistence is approached [26–28]. However, elastic effects appear only extremely close to coexistence, i.e., in fairly thick wetting layers and, within a Landau–de Gennes model, give rise to a surface phase transition taking place just before coexistence which separates nematic films with uniform director from nematic films with a linearly distorted director [28]. We anticipate that the study of these effects by density-functional theory will be difficult since one needs a very fine control over the bulk conditions of the system and their departure from coexistence.

In order to explore this transition using our density-functional model we tried to follow an approach similar to that used in Ref. [28], where the free-energy functional is minimized with respect to all variables except the slow ones, i.e., the thickness of the wetting layer L and the tilt angle at the NI interface, ψ_{NI} (assuming strong anchoring conditions at the substrate, $\psi = 0°$, and a linear behavior of the director distortion, ψ_{NI} defines the degree of distortion of the director across the wetting layer). Thus we conducted constrained minimizations to compute an effective surface free energy $\gamma_{SI}^{*}(L, \psi_{NI})$ for the SI interface (incidentally, the constrained minimization produces numerically similar results if the minimization is not constrained at all but allowed only for a limited number of iterations, this number being sufficient to relax the rapid, short-length scale variables; this is in practice the methodology that we tried to use). In these minimizations, the tilt-angle profile was set initially to a linear function of z, and the density and uniaxial and biaxial order parameters were set to the corresponding bulk values. Once this effective surface free energy is obtained, it can be minimized in a separate process with respect to L and ψ_{NI}. However, this program failed since the minimization process leading to the construction of $\gamma_{SI}^{*}(L, \psi_{NI})$ becomes terribly painful due to computer time limitations. Some estimates based on elastic theory indicate that the critical nematic film thickness for which elastic effects would begin to be favorable with respect to boundary effects is $\sim 100\sigma_{\text{eq}}$, which is outside our present computational capabilities. However, full density-functional calculations of films with thicknesses less and larger than this value give an indirect indication that there must be a phase transition between two phases with uniform

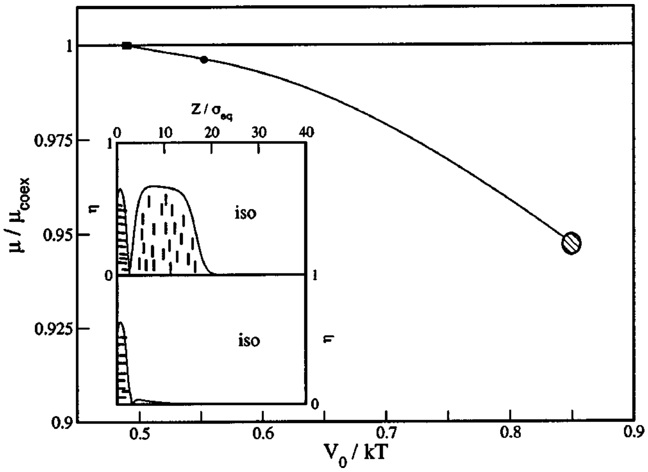

FIG. 6. Prewetting phase diagram in the chemical potential μ and surface strength parameter V_0 plane. The surface potential decay inverse length is taken to be $\alpha=0.3\sigma_{\mathrm{eq}}^{-1}$. The coexistence line is represented by a horizontal axis; the filled square on this line indicates the wetting transition by nematic with parallel director alignment, $V_0^{N\parallel}$. The thin line starting at $V_0^{N\parallel}$ is the prewetting transition line, which ends in a critical point indicated by a big circle. The insets show the uniaxial order-parameter profiles of two films that coexist on the prewetting line at the point shown by a filled circle. Molecular orientations in the films are drawn, and the bulk isotropic phase is indicated by "iso."

director configuration and distorted director, respectively, since in the first (second) case the distorted-tilt-angle configuration is seen to be less (more) stable than a film having a uniform director configuration.

2. Wetting by a nematic with director parallel to the susbstrate

When the surface strength parameter V_0 is sufficiently high there occurs a new wetting transition where the director of the nematic film is uniformly oriented parallel to the substrate (see Fig. 2). No distorted director configurations arise here since the boundary conditions at the two interfaces, namely, the substrate and the isotropic-nematic interfaces, are both satisfied. This time the wetting transition is clearly of first order, as evidenced by the large jump in nematic adsorption that occurs at the wetting transition, $V_0=V_0^{WN\parallel}\equiv 0.478kT$. Further evidence of the first-order character of the transition is obtained by analyzing the occurrence of an off-coexistence prewetting line separating two films of different thicknesses, which is a necessary thermodynamic consistency condition. As expected, the prewetting line is very close to coexistence. Figure 6 shows a μ vs V_0 phase diagram where the coexistence line is represented by the horizontal axis on which a point, represented by a filled square, indicates the location of the wetting transition $V_0^{WN\parallel}$, separating wetting from nonwetting states. The thin line starting at this point and separating tangentially from the coexistence line is the prewetting line. As usual, this line is seen to exist extremely close to coexistence (see the chemical potential scale) and to end in a surface critical point (V_0^{PW},μ^{PW}) where both films become the same and whose location we have not estimated with any accuracy [the point shown merely indicates that beyond that point no sharp transition could be found; a method based on extrapolation using a power law for the difference in nematic adsorption between the two films $\Delta\Gamma\sim(\mu-\mu^{PW})^{\beta}$ proved numerically unreliable due to the impossibility to obtain good-quality estimates of adsorption to be used in the extrapolation]. The figure includes as insets the uniaxial order-parameter profiles (and the typical molecular configurations, indicated by short segments) of two particular films that coexist on the prewetting line at the point indicated by a filled circle; note that in this range of values of the surface strength V_0 there persists a first molecular layer with homeotropic orientation but the prewetting transition occurs between thicker films with parallel orientation.

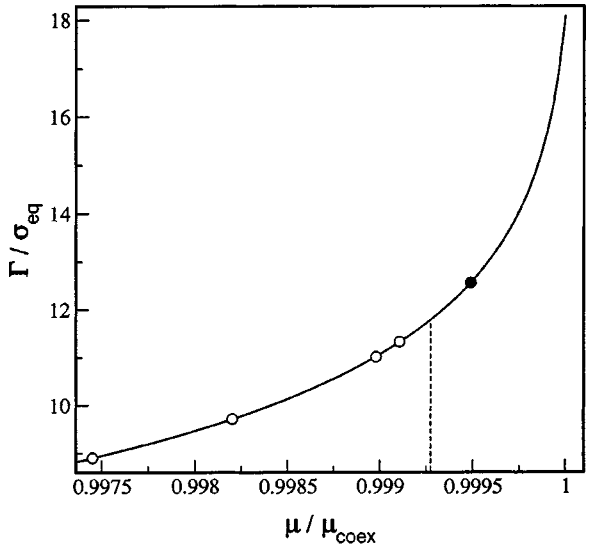

FIG. 7. Nematic-adsorption Γ vs chemical potential μ relative to the coexistence value μ_{coex} for a substrate strength parameter $V_0=0.5kT$ and a surface potential decay inverse length $\alpha=0.3\sigma_{\mathrm{eq}}^{-1}$ to the substrate. The data are associated to the wetting transition at $V_0^{WN\parallel}$ of a nematic with the director aligned parallel to the substrate. Symbols are calculations with the density functional. The filled circle corresponds to a stable thick film. The open circles are metastable thick films. Continuous lines are fits to the form $\Gamma=a+b\,\ln(\mu/\mu_{\mathrm{coex}}-c)$. The dashed vertical line indicates the location of the prewetting transition.

The nematic-adsorption parameter is plotted in Fig. 7 for $V_0=0.5kT>V_0^{WN\parallel}$ as $\mu\rightarrow\mu_{\mathrm{coex}}^{-}$. Note that for this value of V_0 there is a prewetting transition prior to the bulk wetting transition; this is indicated in the figure by the vertical line. Data represented by open circles are metastable states corresponding to metastable thick films (adsorption data for the thin films are much too low for them to be seen in the figure), whereas the filled circle is an equilibrium thick film. The data in the graph have been fitted to a logarithmic law of the form $\Gamma=a+b\,\ln[(c-x)/x]$, with $x=V_0/kT$. The fitting parameters obtained were $a=-5.38\sigma_{\mathrm{eq}}$, $b=2.39\sigma_{\mathrm{eq}}$, and $c=1.00$ The value for the amplitude of the logarithm, *b*, is numerically very similar in both wetting transitions. This was to be expected since, in the true asymptotic régime, the amplitude of the logarithm must be equal to the correlation length of the bulk nematic phase.

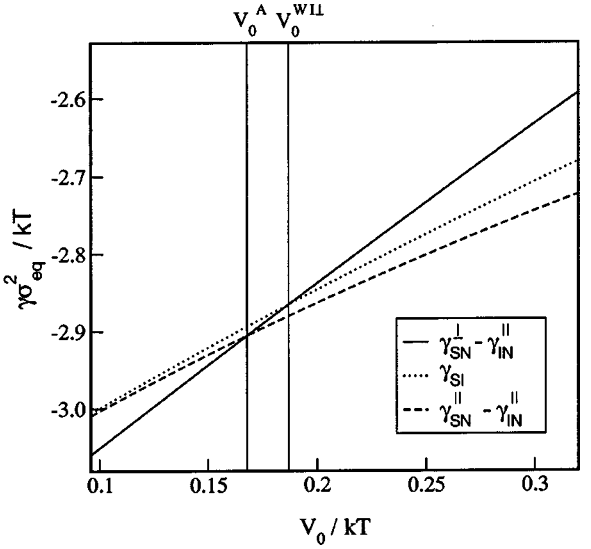

FIG. 8. Surface tensions γ of the different interfaces as a function of surface strength parameter V_0 in the region of partial wetting. The surface potential decay inverse length is taken to be $\alpha = 0.3\sigma_{\mathrm{eq}}^{-1}$. The surface tensions for the interfaces involved in the (metastable) wetting transition by the isotropic phase ($\gamma_{SN}^{\parallel}$ for the substrate-nematic interface with the director oriented parallel to the substrate, $\gamma_{SN}^{\perp}$ for the substrate-nematic interface with the director oriented perpendicular to the substrate, γ_{SI} for the substrate-isotropic interface, and $\gamma_{IN}^{\parallel}$ for the equilibrium free-nematic-isotropic interface with director parallel to the interface) are represented by lines, as indicated in the key box. The appropriate nematic-isotropic surface tension is subtracted from γ_{SI} to permit easier visualization of the wetting transition by isotropic, indicated in the upper part of the panel by $V_0^{WI\perp}$, and the anchoring transition, indicated by V_0^A (the corresponding wetting transition by isotropic $V_0^{WI\parallel}$ is not shown in the figure).

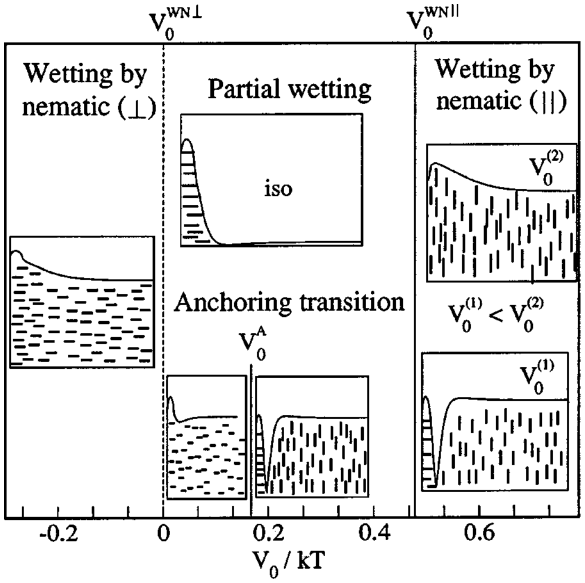

FIG. 9. Summary of the wetting phenomenology found for the system studied. The horizontal axis is the surface strength parameter V_0. The first wetting transition by nematic is denoted by $V_0^{WN\perp}$, below which a nematic phase wets the substrate with the director perpendicular to the substrate. As indicated by the dashed vertical line, this transition appears to be of second order. The second wetting transition by nematic is denoted by $V_0^{WN\parallel}$; above this a nematic phase wets the substrate with the director parallel to the substrate. As indicated by the continuous vertical line, this transition is of first order. In this case, depending on the value of V_0, a first layer with molecules oriented perpendicular to the director occurs or not. In the region $V_0^{WN\perp} < V_0 < V_0^{WN\parallel}$ partial wetting occurs. In this region a first-order anchoring transition takes place at V_0^A, separating phases with different director orientation sufficiently far from the substrate.

B. Anchoring transition

As can be seen in Fig. 2 the surface tensions $\gamma_{SN}^{\perp}$ and $\gamma_{SN}^{\parallel}$ cross at a value $V_0 = V_0^A \equiv 0.168kT$, indicating that, on increasing V_0, the nematic director far from the substrate no longer orients perpendicular to the substrate but adopts a parallel configuration. This is an anchoring transition from homeotropic to parallel alignment. Note that here there also appears a first layer where the molecules still anchor with perpendicular orientation; we remind the reader that this layer arises from the strong tendency of the HSPC molecules to pack together near the substrate with their axes perpendicular to the surface. Therefore, the first layer plays a major role in the occurrence of this transition, which appears as a competition between the orienting dispersion force due to the substrate, favoring parallel ordering, and the purely entropic field due to the first layer which is exerted on the fluid next to it, which favors homeotropic ordering.

C. Wetting by the isotropic phase

Wetting by the isotropic phase also occurs in this system, but it always happens to be metastable. To see this appropriate surface tensions have been represented in Fig. 8. The anchoring transition, separating nematic films with homeotropic and parallel orientations, is again indicated. For values $V_0 > V_0^A$ the equilibrium substrate-nematic interface consists of a nematic director parallel to the substrate. However, at $V_0 = V_0^{WI\perp} \equiv 0.187kT$ the *metastable* substrate-nematic interface with director perpendicular to the substrate undergoes a wetting transition at which an infinitely thick isotropic film intrudes between the substrate and the nematic phase. For values $V_0 < V_0^A$ the equilibrium substrate-nematic interface consists of a nematic director perpendicular to the substrate but, at $V_0 = V_0^{WI\parallel}$ (not shown in the figure), the *metastable* substrate-nematic interface with director parallel to the substrate undergoes a wetting transition at which an infinitely thick isotropic film intrudes between the substrate and the nematic phase. Note that, in both cases once the isotropic film has wet the substrate, the bulk nematic director aligns parallel to the substrate, as it corresponds to the equilibrium free-NI interface. These two metastable transitions are both of first order. The sense in which these transitions are called metastable is the following. We assume the hypothetical situation where the bulk nematic phase may reaccommodate the director orientation and that this is driven by the behavior at the SN interface or at the NI once the latter is depinned from the substrate. Implicitly this is equivalent to assuming that no other interfaces compete by establishing new preferred axes.

If this is not the case the wetting transitions discussed in this section could indeed be realized, since the anchoring transition could be suppressed and the preferred orientation at the NI interface imposed by suitable strong anchoring conditions at other interfaces.

IV. CONCLUSIONS

To conclude, we have examined the wetting behavior of a fluid of hard spherocylinders in contact with a model substrate. By changing the affinity of the substrate toward differently oriented nematics distinct wetting behaviors are observed. In particular, as the strength of the surface interactions is increased we observe wetting by a homeotropically aligned nematic, nonwetting, and wetting by a parallel-aligned nematic film. As observed in simple isotropic fluids, the nature of the wetting phase transitions crucially depends on the range of the surface interactions. Thus, whereas the wetting transition of homeotropic films is of second order, for parallel-aligned films we find a first-order transition and an associated prewetting line off coexistence that ends in a surface critical point. In addition, an anchoring transition has been found between films with homeotropic and parallel alignments. All these features, collected graphically in Fig. 9, imply that the HSPC model exhibits an extremely rich surface behavior making it an appropriate model to incorporate other more realistic features in the intermolecular potentials such as van der Waals or electrostatic forces. These studies, together with the analysis of behavior in confined geometries, will be left for future work.

ACKNOWLEDGMENTS

This work was partially supported by Grant Nos. BFM2001-0224-C02-01, BFM2001-0224-C02-02, and BFM2001-1679-C03-02 (Spain). D. de las H. is supported by a FPU grant from The Spanish Ministry of Education and Culture.

---

[1] P. Sheng, Phys. Rev. Lett. **37**, 1059 (1976); Phys. Rev. A **26**, 1610 (1982).

[2] T.J. Sluckin and A. Poniewierski, Phys. Rev. Lett. **55**, 2907 (1985).

[3] T.J. Sluckin and A. Poniewierski, in *Fluid Intefacial Phenomena*, edited by C. A. Croxton (Wiley, Chichester, 1986), Chap. 5, and references therein.

[4] A. Poniewierski and A. Samborski, J. Chem. Phys. **105**, 7632 (1996).

[5] G.D. Wall and D.J. Cleaver, Phys. Rev. E **56**, 4306 (1997).

[6] M.P. Allen, Mol. Phys. **96**, 1391 (1999).

[7] M.P. Allen, J. Chem. Phys. **112**, 5447 (2000).

[8] A. Poniewierski and R. Holyst, Phys. Rev. A **38**, 3721 (1988).

[9] A. Poniewierski, Phys. Rev. E **47**, 3396 (1993).

[10] R. Zwanzig, J. Chem. Phys. **39**, 1714 (1963).

[11] R. van Roij, M. Dijkstra, and R. Evans, J. Chem. Phys. **113**, 7689 (2000).

[12] M. Dijkstra, R. van Roij, and R. Evans, Phys. Rev. E **63**, 051703 (2001).

[13] A.M. Somoza and P. Tarazona, Phys. Rev. Lett. **61**, 2566 (1988); J. Chem. Phys. **91**, 517 (1989).

[14] E. Velasco, L. Mederos, and D.E. Sullivan, Phys. Rev. E **62**, 3708 (2000).

[15] E. Velasco, L. Mederos, and D.E. Sullivan, Phys. Rev. E **66**, 021708 (2002).

[16] L. Onsager, Ann. N.Y. Acad. Sci. **51**, 627 (1949).

[17] J.D. Parsons, Phys. Rev. A **19**, 1225 (1979).

[18] S.-D. Lee, J. Chem. Phys. **87**, 4972 (1987); **89**, 7036 (1988).

[19] R. Holyst and A. Poniewierski, Phys. Rev. A **38**, 1527 (1988).

[20] R. Holyst, Mol. Phys. **68**, 391 (1989).

[21] J.R. Henderson, in *Fundamentals of Inhomogeneous Fluids*, edited by D. Henderson (Marcel Dekker, New York, 1992), Chap. 2.

[22] B.G. Moore and W.E. McMullen, Phys. Rev. A **42**, 6042 (1990).

[23] Z.Y. Chen and J. Noolandi, Phys. Rev. A **45**, 2389 (1992).

[24] Z.Y. Chen, Phys. Rev. E **47**, 3765 (1993).

[25] Angular integrations are computed using numerical quadrature. As a result, the value of the excluded-volume term, involving integrals over $\hat{\mathbf{\Omega}}$ and $\hat{\mathbf{\Omega}}'$, depends very weakly on the tilt angle of the director, ψ (this is not correct, since the free energy of the nematic phase should be invariant with respect to the orientation of the director, hence the tilt angle). When calculating bulk coexistence between the isotropic and nematic phases, the coexistence chemical potential $\mu_{\rm coex}$ and pressure P turn out to depend slightly on the tilt angle. If nematic regions with different tilt angles are adsorbed on the substrate there is an inconsistency as to which value of $\mu_{\rm coex}$ and Ω_b should be used. Even though the effect is unimportant as long as the chemical potential corresponds to the bulk nematic phase with the chosen tilt angle, we have introduced, for the sake of consistency, a local chemical potential and a local pressure that depend linearly on the tilt angle between $\psi=0°$ and $\psi=90°$.

[26] D.E. Sullivan and R. Lipowsky, Can. J. Chem. **66**, 553 (1988).

[27] T.J. Sluckin and A. Poniewierski, Mol. Cryst. Liq. Cryst. **179**, 349 (1990).

[28] N. Braun, T.J. Sluckin, and E. Velasco, J. Phys.: Condens. Matter **8**, 2741 (1996).